Quaternary Selenophosphate $Cs_2ZnP_2Se_6$ Featuring Unique One-dimensional Chains and Exhibiting Remarkable Photo-electrochemical Response①

LI Meng-Yue[a, b] XIE Xiu-Yuan[a, b] WU Xin-Tao[b]
LI Xiao-Fang[b②] LIN Hua[b②]

[a] (*Department of Chemistry, Fuzhou University, Fuzhou* 350116, *China*)

[b] (*State Key Laboratory of Structural Chemistry, Fujian Institute of Research on the Structure of Matter, Chinese Academy of Sciences, Fuzhou* 350002, *China*)

ABSTRACT New functional materials of metal chalcophosphates have been receiving increasing attention due to their wide structural diversity and technologically promising properties. In this work, a quaternary selenophosphate, $Cs_2ZnP_2Se_6$, has been successfully prepared by the high-temperature solid state reactions with a modified reactive CsCl flux. Single-crystal X-ray diffraction analyses show that $Cs_2ZnP_2Se_6$ crystallizes in triclinic space group $P\bar{1}$ with a = 7.66000(10), b = 7.712(7), c = 12.7599(3) Å, α = 96.911(18)°, β = 104.367(14)°, γ = 109.276(13)°, V = 672.16 Å^3 and Z = 2. The major structure feature is the one-dimensional (1*D*) chain comprised of alternating units of tetrahedrally coordinated Zn^{2+} ions to the ethane-like $[P_2Se_6]^{4-}$ units, in which counterbalanced Cs cations are accommodated. Significantly, photo-electrochemical measurement indicated that the title compound was photo-responsive under visible-light illumination. Moreover, the optical gap of 2.67 eV for $Cs_2ZnP_2Se_6$ was deduced from the UV/Vis reflectance spectroscopy and theoretical calculation shows an indirect band gap with an electronic transfer excitation of Se-4*p* to Zn-3*d*/4*p* and P-3*p* orbitals. This work presents not only a novel potential application of metal chalcophosphates, but also a facile approach to prepare alkali metal-containing chalcogenides.

Keywords: selenophosphate, zinc, one-dimensional chain, photo-electrochemistry, semiconductor;
DOI: 10.14102/j.cnki.0254–5861.2011–2822

1 INTRODUCTION

As an important component of multifunctional materials, metal chalcophosphates have been receiving increasing attention for their potential applications in reversible phase-change transitions[1, 2], ferroelectricity[3, 4], nonlinear optics[5–8], photoluminescence[9], γ-ray detection[10], thermoelectrics[11], and magnetism[12]. In terms of structure, $[P_xQ_y]^{z-}$ anion groups are formed by tetrahedral or pyramidal phosphorus and some have complex structures such as (1*D*) $[P_2Q_6]^{2-}$[7, 9, 12, 15], $[PQ_6]^{-}$[8, 11, 14], $[P_3Q_4]^{-}$[13], $[P_5Q_{10}]^{5-}$[16–18], and zero-dimensional (0*D*) $[PQ_4]^{3-}$[10, 19, 20], $[P_2Q_6]^{4-}$[21–23], $[P_2Q_9]^{4-}$[24], $[P_2Q_{10}]^{4-}$[25], $[P_3Q_7]^{3-}$[26], $[P_5Q_{12}]^{5-}$[5], $[P_6Q_{12}]^{4-}$[5, 27] and $[P_8Q_{18}]^{6-}$[28]. In the case of selenium, the ethane-like $[P_2Se_6]^{4-}$ units are the most dominant building block[15]. Furthermore, these $[P_2Se_6]^{4-}$ units coordinate with metal atoms to form structures of different dimensions. Typical examples include 0*D* $M^{II}{}_2P_2Se_6$ (M^{II} = Ba, Ca, Eu, Pb, Sn, Sr)[29–31] and $M^{I}{}_4P_2Se_6$ (M^{I} = Ag, K, Na, Tl)[19, 32–34]; 1*D* $A_2P_2Se_6$ (A = K, Rb)[7], $A_2M^{I}{}_2P_2Se_6$ (A = K, Cs; M^{I} = Cu, Ag, Au)[20, 22], $KInP_2Se_6$[35], $K_4Sc_2(PSe_4)_2(P_2Se_6)$[36], $K_4In_2(PSe_5)_2(P_2Se_6)$[37], $Rb_3Sn(PSe_5)(P_2Se_6)$[37], $K_5In_3P_6Se_{19}$[38], $K_4In_4P_6Se_{20}$[38] and $Rb_2M^{III}P_2Se_7$ (M^{III} = Ce, Gd)[39]; two-dimensional (2*D*) $NaCeP_2Se_6$[40], $K_2LaP_2Se_7$[41], $Rb_4Sn_5P_4Se_{20}$[42], $Cs_4ThP_5Se_{17}$[43], $M^{II}{}_2P_2Se_6$ (M^{II} = Fe, Hg, Mg, Zn)[23, 44, 45], KMP_2Se_6 (M = Sb, Bi)[46], and $A_2ThP_3Se_9$ (A = K, Rb)[43]; and three-dimensional (3*D*) $K_{10}Sn_3(P_2Se_6)_4$[47] and $KREP_2Se_6$ (RE = Y, La, Ce, Pr, Gd)[12].

Received 25 March 2020; accepted 8 April 2020 (**CCDC 1976181**)

① This research was supported by the National Natural Science Foundation of China (21771179 and 21301175) and the Natural Science Foundation of Fujian Province (2019J01133)

② Corresponding authors. Li Xiao-Fang and Lin Hua. E-mails: lixiaofang@fjirsm.ac.cn and linhua@fjirsm.ac.cn

To date, most metal chalcophosphates containing alkali metals have been prepared by the traditional solid-state reactions at high temperature using the molten alkali metal polychalcogenide flux techniques[48]. Recently, we have used the alkali metal halide mixtures as reactive fluxes and this synthetic approach appears to be of general utility in preparing new multinary chalcogenides with various alkali metals[49–69].

With the above considerations in mind, we focused our investigations on the quaternary A/M/P/Q system and successfully obtained one Zn-containing chalcophosphate, $Cs_2ZnP_2Se_6$. Crystal structure of this compound was first characterized by Kanatzidis et al. in 2016, but there were not any physicochemical properties reported[70]. In this paper, the synthesis, optical gap and theoretical calculation are systemically presented. Moreover, photo-responsive under visible-light illumination are discovered in the metal chalcophosphate for the first time.

2 EXPERIMENTAL

2. 1 Synthesis of $Cs_2ZnP_2Se_6$

All manipulations were performed in a dry Ar-filled glovebox (H_2O content < 0.1 ppm, O_2 content < 0.1 ppm). Se (99.999%, Aladdin), P (99%, ABCR), Zn (99.95%, Alfa-Aesar) and CsCl (99.99%, Aladdin) were used as received. $Cs_2ZnP_2Se_6$ was prepared from a mixture of CsCl, Zn, P, and Se in the molar ratio of 1.75:2:4:9. The reactants were loaded into a silica crucible and then transferred into a silica jacket. This jacket was flame sealed under a vacuum of 10^{-3} Pa, and then heated in a tube furnace from room temperature to 723 K in 20 h and annealed at this temperature for 20 h, and then heated to 1173 K at a rate of 20 K/h, following a hold time of 50 h, finally subsequently cooled to 573 K at 5 K/h before the furnace was turned off. After washing with distilled water and absolute ethanol, the products consisting of yellow rods of the title compound were obtained. Based on the single-crystal X-ray structural analysis and energy dispersive X-ray spectroscope (EDX) elemental results (Fig. 1), the chemical formula "$Cs_2ZnP_2Se_6$" was given. The homogeneity of samples was obtained as indicated by the powder X-ray diffraction data (PXRD) shown in Fig. 2. The title compound was insoluble in water and stable in air for more than two months.

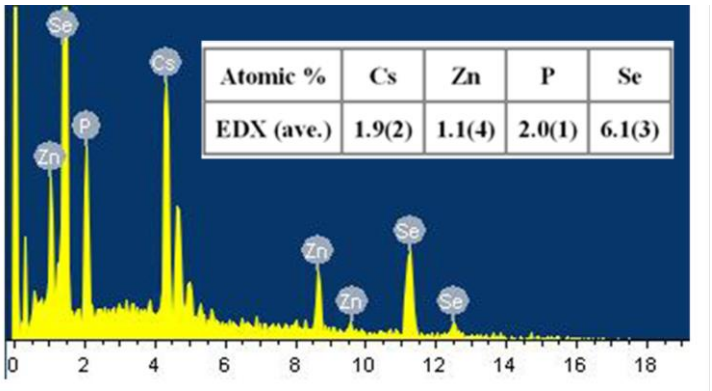

Atomic %	Cs	Zn	P	Se
EDX (ave.)	1.9(2)	1.1(4)	2.0(1)	6.1(3)

Fig. 1. EDX results of $Cs_2ZnP_2Se_6$

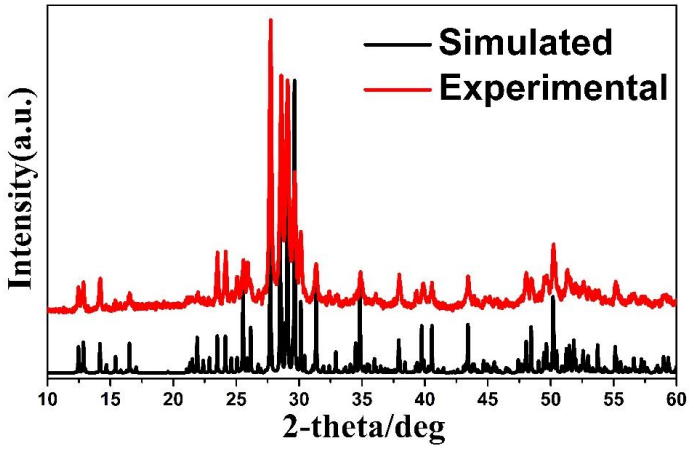

Fig. 2. Experimental (red) and simulated (black) PXRD patterns of $Cs_2ZnP_2Se_6$

2. 2 Single-crystal X-ray crystallography determination

A yellow rod-shaped crystal was mounted on a glass fiber. The single-crystal X-ray diffraction data were collected on a Rigaku Mercury CCD diffractometer equipped with a graphite-monochromated Mo-*Ka* radiation source (λ = 0.71073 Å) at 293 K. The data were corrected for Lorentz and polarization factors. Absorption correction was performed by the multi-scan method[71]. The structure was solved by direct methods and refined by full-matrix least-squares fitting on F^2 by SHELXL-2014[72]. All atoms were refined with anisotropic thermal parameters. The coordinates were standardized using STRUCTURE TIDY[73]. The structure was solved and refined successfully in the triclinic $P\bar{1}$ space group with a = 7.66000(10), b = 7.712(2), c = 12.7599(3) Å, α = 96.911(18)º, β = 104.367(14)º, γ = 109.276(13)º, V = 672.16(3) Å^3 and Z = 2. The final R = 0.0416 and wR = 0.0998 ($w = 1/[\sigma^2(F_o^2) + (0.0443P)^2 + 8.7453P]$, where $P = (F_o^2 + 2F_c^2)/3$), $(\Delta\rho)_{max}$ = 1.598, $(\Delta\rho)_{min}$ = −1.529 and S = 1.029 for 3045 observed reflections ($I > 2\sigma(I)$) with 151 parameters and generated a formula of $Cs_2ZnP_2Se_6$, which agreed well with the EDX results. The parameters of atomic positions and anisotropic displacement are shown in Table 1. The selected key lengths are listed in Table 2.

Table 1. Atomic Coordinates and Equivalent Isotropic Displacement Parameters of $Cs_2ZnP_2Se_6$

Atom	Wyckoff	*x*	*y*	*z*	U_{eq}
Cs(1)	2*i*	0.59588(8)	0.30056(8)	0.39350(5)	0.03057(18)
Cs(2)	2*i*	0.74098(9)	0.40652(8)	0.09823(5)	0.03269(18)
Zn	2*i*	0.03063(14)	0.95519(14)	0.25107(7)	0.0227(3)
P(1)	2*i*	0.1055(3)	0.1506(3)	0.52976(16)	0.0177(4)
P(2)	2*i*	0.1608(3)	0.0846(3)	0.03742(17)	0.0183(4)
Se(1)	2*i*	0.03664(13)	0.72401(12)	0.36888(7)	0.0234(2)
Se(2)	2*i*	0.09275(13)	0.25693(12)	0.37598(7)	0.0212(2)
Se(3)	2*i*	0.22160(14)	0.36214(13)	0.12947(7)	0.0273(2)
Se(4)	2*i*	0.25693(13)	0.91426(13)	0.14879(7)	0.0233(2)
Se(5)	2*i*	0.38947(13)	0.17818(14)	0.62399(8)	0.0295(2)
Se(6)	2*i*	0.27516(12)	0.08627(13)	0.89457(7)	0.0225(2)

[a] U_{eq} is defined as one-third of the trace of the orthogonalized U_{ij} tensor

Table 2. Selected Bond Lengths (Å) of $Cs_2ZnP_2Se_6$

Bond	Dist.	Bond	Dist.
Cs(1)−Se(1)	3.6616(12)	Cs(2)−Se(6)	3.7742(10)
Cs(1)−Se(2)	3.7033(10)	Cs(2)−Se(6)	3.9448(10)
Cs(1)−Se(5)	3.7121(11)	Cs(2)−Se(3)	4.0032(11)
Cs(1)−Se(4)	3.7413(14)	Zn−Se(1)	2.4708(13)
Cs(1)−Se(5)	3.7458(11)	Zn−Se(2)	2.4862(14)
Cs(1)−Se(2)	3.8360(14)	Zn−Se(4)	2.4886(12)
Cs(1)−Se(1)	3.9567(12)	Zn−Se(6)	2.4989(14)
Cs(1)−Se(2)	3.9873(10)	P(1)−Se(5)	2.135(2)
Cs(1)−Se(5)	4.0189(11)	P(1)−Se(2)	2.208(2)
Cs(1)−Se(3)	4.0356(13)	P(1)−Se(1)	2.210(2)
Cs(2)−Se(3)	3.6096(11)	P(1)−P(1)	2.252(4)
Cs(2)−Se(1)	3.6706(14)	P(2)−Se(3)	2.155(2)
Cs(2)−Se(6)	3.6905(14)	P(2)−Se(4)	2.203(2)
Cs(2)−Se(3)	3.7371(11)	P(2)−Se(6)	2.209(2)
Cs(2)−Se(4)	3.7721(12)	P(2)−P(2)	2.257(4)

2. 3 Powder X-ray diffraction (PXRD)

Powder X-ray diffraction (PXRD) patterns were collected on a Rigaku MiniFlex II powder diffractometer by using Cu-$K\alpha$ radiation at room temperature. The measurement range of 2θ is 10～70° and the scan step width was 0.02°.

2. 4 Elemental analysis

The elemental analysis data were collected on a field emission scanning electron microscope (FESEM, JSM6700F) equipped with an energy dispersive X-ray spectroscope (EDX, Oxford INCA) on clean single crystal surfaces.

2. 5 UV-Vis-near IR spectroscopy

The optical diffuse reflectance spectra of $Cs_2ZnP_2Se_6$ powdery samples were measured by a Perkin-Elmer Lambda 950 UV-vis spectrometer equipped with an integrating sphere over a 200～2000 nm wavelength range at room temperature and a $BaSO_4$ plate as a reference, on which the finely ground sample powders were coated. The absorption spectrum was calculated using the Kubelka-Munk function: $\alpha/S = (1 - R)^2/2R$ (α: absorption coefficient, S: scattering coefficient, R: reflectance)[74].

2. 6 Photocurrent measurement

To investigate the optical behavior of $Cs_2ZnP_2Se_6$, a photo-electrochemical cell consisting of three electrodes (A glassy carbon electrode (GCE, 3.00 mm in diameter), saturated Ag/AgCl electrode and Pt wires were served as the working electrode, reference electrode and counter electrode, respectively) was constructed. Then, the reaction was carried out by irradiating the solution using a 300 W Xe lamp (PLS-SXE300CUV, $\lambda > 420$ nm). And the result of the transient photocurrent was recorded by a CHI660E electrochemical workstation (Shanghai Chen-Hua Instrument Corporation, China) at 298 K in 1.0 M KOH (aq) electrolyte.

2. 7 Computational methods

Utilizing density functional theory (DFT) as implemented in the Vienna *ab-initio* simulation package (VASP) code[75], we investigate the electronic structures of the title compound. We used projector augmented wave (PAW) method[76] for the ionic cores and the generalized gradient approximation (GGA)[77] for the exchange-correlation potential, in which the Perdew-Burke-Ernzerhof (PBE) type[78] exchange-correlation was adopted. The reciprocal space was sampled with 0.03 $Å^{-1}$ spacing in the Monkhorst-Pack scheme for structure optimization, while denser k-point grids with 0.01 $Å^{-1}$ spacing were adopted for property calculation. We used a mesh cutoff energy of 600 eV to determine the self-consistent charge density. All geometries are fully relaxed until the Hellmann-Feynman force on atoms is less than 0.01 eV/Å and the total energy change is lower than 1.0×10^{-5} eV.

3 RESULTS AND DISCUSSION

3. 1 Structure description

Single-crystal XRD data reveal that compound $Cs_2ZnP_2Se_6$ crystallizes in the triclinic space group $P\bar{1}$ (No. 2) with a = 7.66000(10), b = 7.712(7), c = 12.7599(3) Å, α = 96.911(18)°, β = 104.367(14)°, γ = 109.276(13)°, V = 672.16 $Å^3$ and Z = 2. In a symmetric unit, there are 11 crystallographically unique atoms, including two Cs (Cs(1), Cs(2)) sites, one Zn site, two P (P(1), P(2)) sites and six Se (Se(1), Se(2), Se(3), Se(4), Se(5), Se(6)) sites, respectively, and all of them are at the Wyckoff sites of 2i. The detailed refinement data are listed in Table 1, and the selected bond distances are shown in Table 2.

The crystal structure is shown in Fig. 3, in which the 1D chain structure is composed of $[ZnP_2Se_2]^{2-}$ chains extending along the c axis and scattering with Cs cations located in the chains. Two types of ethane-like structures where the $[P_2Se_6]^{4-}$ group ($[(P1)_2Se_6]^{4-}$ and $[(P2)_2Se_6]^{4-}$) and the $[ZnSe_4]^{6-}$ group with four different bond lengths intersect and share Se atoms make this 1D $[ZnP_2Se_2]^{2-}$ anion chain. The Zn^{2+} ions form 4-fold tetrahedral $[ZnSe_4]$ containing one Se(1), one Se(2), one Se(4) and one Se(6) atoms. As depicted in Fig. 4, the Zn atom shows usual Zn–S interatomic lengths, ranging from 2.4708(13) to 2.4989(14) Å. P(1) atom bridges with P(1) atom to form a P−P bond in 2.252 Å, and each P(1) atom forms a bond with three Se atoms. Similarly, two P(2) atoms form a P–P bond with a bond length of 2.257, and each P(2) atom and the surrounding Se atoms form a tri-coordination environment. The P atom shows the customary P–Se interatomic lengths, ranging from 2.135(2) to 2.210(2) Å. The Cs(1) cation has a coordination environment with ten Se atoms, while Cs(2) cation coordinates with eight Se atoms. For all this, the Cs–Se distances vary from 3.6096(11) to 4.0356(13) Å, which is common in $CsSbSe_2$ (3.570 ～ 4.222 Å)[79], $Cs_8Ga_4Se_{10}$ (3.379～4.268 Å)[80] and $Cs_{10}Ga_6Se_{14}$ (3.444～4.329 Å)[80].

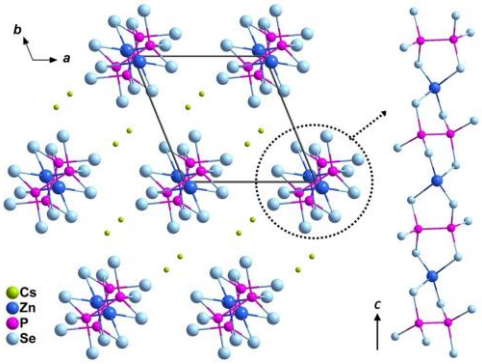

Fig. 3. Structure view of $Cs_2ZnP_2Se_6$ viewed down the *c*-direction with the unit cell marked (left). A single 1*D* chain built of corner sharing [P_2Se_6] and [$ZnSe_4$] units (right)

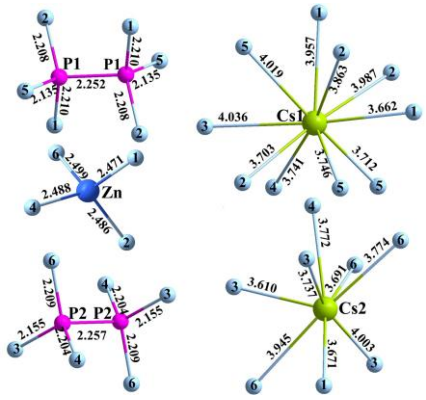

Fig. 4. Basic building units of [$(P(1))_2Se_6$], [$ZnSe_4$], [$(P(2))_2Se_6$], [$Cs(1)Se_{10}$] and [$Cs(2)Se_{10}$] in $Cs_2ZnP_2Se_6$ with the atom numbers and bond lengths marked

3. 2 Optical properties

The optical absorption spectrum (Fig. 5) shows the band gap (E_g) is 2.67 eV for $Cs_2ZnP_2Se_6$, which is consistent with its yellow color. Such value is well-consistent with the previously reported result in $Cs_2ZnP_2Se_6$ (E_g = 2.63 eV) by Kanatzidis et al. in 2016[70]. Moreover, these data are comparable to those of selenophosphates, such as $Cs_5P_5Se_{12}$ (E_g = 2.17 eV)[5], $K_2P_2S_6$ (E_g = 2.08 eV)[7], $CsZrPSe_6$ (E_g = 2.0 eV)[14], and $RbPSe_6$ (E_g = 2.18 eV)][8]. The result of the transient photocurrent in Fig. 6 shows an obvious photocurrent generating when the conductive glass coated with $Cs_2ZnP_2Se_6$ is subjected to excitation with regular visible light. Moreover, the reproducibility of the transient photocurrent response was confirmed by the on-off cycles of illumination. The photocurrent data are around 100 nA/cm^2 that is weaker than those of [$(Ba_{19}Cl_4)(Ga_6Si_{12}O_{42}S_8)$] (150 nA/cm^2)[81] and Lu_5GaS_9 (150 nA/cm^2)[82], but stronger than those of $Yb_6Ga_4S_{15}$ (50 nA/cm^2)[82], $BaCuSbS_3$ (55 nA/cm^2)[83] and $BaCuSbSe_3$ (30 nA/cm^2)[83]. As far as we know, this is the first metal chalcophosphate with remarkable photo-electrochemical response.

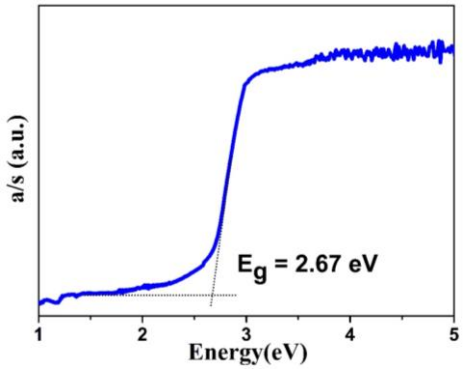

Fig. 5. UV-vis diffuse reflectance of $Cs_2ZnP_2Se_6$

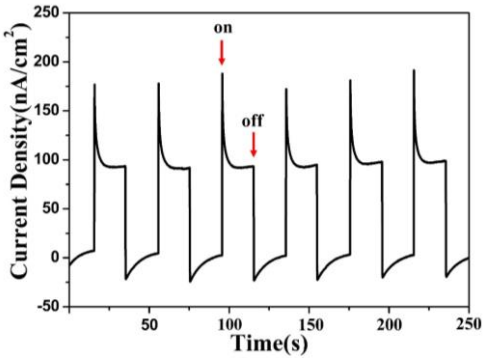

Fig. 6. Transient photocurrent response of $Cs_2ZnP_2Se_6$ under simulated solar light irradiation

3. 3 Electronic structure calculation

The electronic band structure of $Cs_2ZnP_2Se_6$ was calculated and shown in Fig. 7 with the highest occupied state set as E_F = 0 eV. The valence band maximum (VBM) resides at the *Y* point whereas the conduction band minimum (CBM) was found along the *Γ* point. The electronic band structures (Fig. 7) reveals that $Cs_2ZnP_2Se_6$ is an indirect band-gap semiconductor with VBM and CBM at different *k* points. The fundamentally calculated E_g (1.87 eV) is less than the experimental E_g (2.67 eV), which is expected because of the well-known fact that the density functional theory (DFT) underestimates the E_g of bulk solids[84−86].

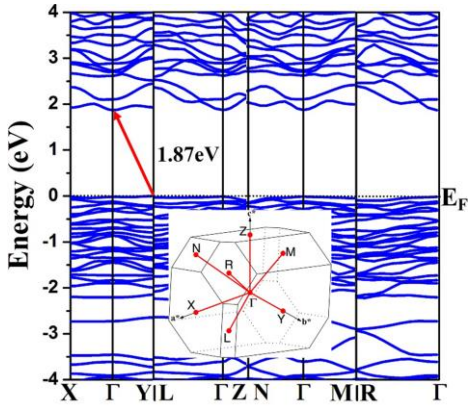

Fig. 7. Calculated electronic band structure of $Cs_2ZnP_2Se_6$. Inset: the first Brillouin zone with symmetry points (red)

Fig. 8 depicts the calculation of partial density of states (PDOS) by the Perdew-Burke-Ernzerhof (PBE). PDOS of Cs, Zn, P, and Se in the energy range of −6～6 eV were divided into four sub-sections VB-I (−6 to −2.5 eV), VB-II (−2.5 to 0 eV), CB-I (1.5 to 4.5 eV), and CB-II (4.5 to 6 eV) according to different orbital features. VB-I has a large contribution from the valence electrons of the P-3*p* and Zn element (4*s* and 3*d* states) that mix with the Se-4*p* states. VB-II is dominated by the *p* orbitals of Zn (4*p*), P (3*p*), and Se (4*p*), indicating that VB-II absorption is not only determined by the charge transitions in $[ZnSe_4]^{6-}$ tetrahedral units but also $[P_2Se_6]^{4-}$ units. The bottom of CB, which contains CB-I and CB-II sections, is primarily derived from Zn element (4*s* and 4*p* states) and P-3*p* and partial P-3*s* especially in the 1.5～4.5 eV energy part with mixing from the Se-4*p* states. As the filling atom, the electron states of Cs contribute only to the higher energy region (4 to 6 eV). Because the optical absorption of a material can be mostly ascribed to the change in transitions between the states of VB and CB near E_g, that is VB-I and CB-I, the $[ZnSe_4]$ and $[P_2Se_6]$ groups should make absolute contributions to the optical properties.

4 CONCLUSION

In summary, by using a facile high-temperature fluxing method, we successfully obtained a quaternary centrosymmetric compound $Cs_2ZnP_2Se_6$, which possesses a one-dimensional $[ZnP_2Se_6]^{2-}$ chain running down the [001] direction separated by isolated Cs^+ cations. UV/Vis/NIR diffuse reflectance spectroscopy study shows its semiconducting behavior with an indirect optical gap of around 2.67

eV conformed by the theoretical study. Significantly, $Cs_2ZnP_2Se_6$ is the first reported metal chalcophosphate with remarkable photo-electrochemical response. These results of this work not only provide a facile approach to prepare alkali metal-containing chalcogenides, but also expand a novel potential application of metal chalcophosphates.

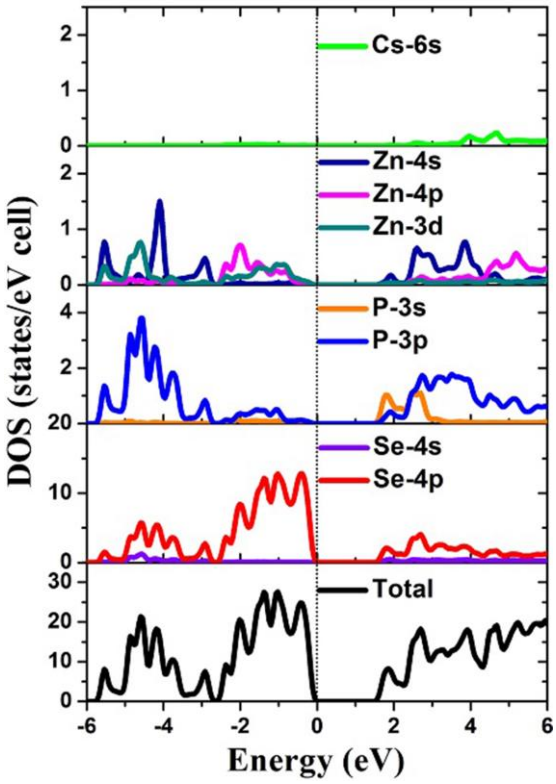

Fig. 8. Total and partial density of states (DOSs) of $Cs_2ZnP_2Se_6$

REFERENCES

(1) Chung, I.; Do, J.; Canlas, C. G.; Weliky, D. P.; Kanatzidis, M. G. $APSe_6$ (A = K, Rb, and Cs): polymeric selenophosphates with reversible phase-change properties. *Inorg. Chem.* **2004**, 43, 2762–2764.

(2) Morris, C. D.; Chung, I.; Park, S.; Harrison, C. M.; Clark, D. J.; Jang, J. I.; Kanatzidis, M. G. Molecular germanium selenophosphate salts: phase-change properties and strong second harmonic generation. *J. Am. Chem. Soc*. **2012**, 134, 20733–20744.

(3) Vysochanskii, Y. Ferroelectricity in complex chalcogenides M′M′′P_2X_6 (M′, M′′ = Sn, Pb, Cu, In, Cr; X = S, Se). *Ferroelectrics* **1998**, 218, 275–282.

(4) Ok, K. M.; Chi, E. O.; Halasyamani, P. S. Bulk characterization methods for non-centrosymmetric materials: second-harmonic generation, piezoelectricity, pyroelectricity, and ferroelectricity. *Chem. Soc. Rev*. **2006**, 35, 710–717.

(5) Chung, I.; Jang, J. I.; Gave, M. A.; Weliky, D. P.; Kanatzidis, M. G. Low valent phosphorus in the molecular anions $[P_5Se_{12}]^{5-}$ and β-$[P_6Se_{12}]^{4-}$: phase change behavior and near infrared second harmonic generation. *Chem. Commun*. **2007**, 4998–5000.

(6) Xia, H. P.; Ma, Q. Experimental study on nonlinear-optical property of $Ag_4P_2Se_6$. *J. Alloys Compd*. **2019**, 780, 727–733.

(7) Chung, I.; Malliakas, C. D.; Jang, J. I.; Canlas, C. G.; Weliky, D. P.; Kanatzidis, M. G. Helical polymer $_\infty^2[P_2Se_6]^{2-}$: strong second harmonic generation response and phase-change properties of its K and Rb salts. *J. Am. Chem. Soc*. **2007**, 129, 14996–15006.

(8) Chung, I.; Kim, M. G.; Jang, J. I.; He, J.; Ketterson, J. B.; Kanatzidis, M. G. Strongly nonlinear optical chalcogenide thin films of $APSe_6$ (A = K, Rb) from spin-coating. *Angew. Chem. Int. Ed*. **2011**, 50, 10867–10870.

(9) Breshears, J. D.; Kanatzidis, M. G. β-KMP_2Se_6 (M = Sb, Bi): kinetically accessible phases obtained from rapid crystallization of amorphous precursors. *J. Am. Chem. Soc*. **2000**, 122, 7839–7840.

(10) Wang, P. L.; Liu, Z.; Chen, P.; Peters, J. A.; Tan, G.; Im, J.; Lin, W.; Freeman, A. J.; Wessels, B. W.; Kanatzidis, M. G. Hard radiation detection from the selenophosphate $Pb_2P_2Se_6$. *Adv. Funct. Mater.* **2015**, 25, 4874–4881.

(11) Weldert, K. S.; Zeier, W. G.; Day, T. W.; Panthöfer, M.; Snyder, G. J.; Tremel, W. Thermoelectric transport in Cu_7PSe_6 with high copper ionic mobility. *J. Am. Chem. Soc*. **2014**, 136, 12035−12040.

(12) Chen, J. H.; Dorhout, P. K.; Ostenson, J. E. A comparative study of two new structure types. Synthesis and structural and electronic characterization of K(RE)P_2Se_6 (RE = Y, La, Ce, Pr, Gd). *Inorg. Chem.* **1996**, 35, 5627–5633.

(13) Chondroudis, K.; Kanatzidis, M. G. $_\infty^2[P_2Se_4]^-$: a novel polyanion in $K_3RuP_5Se_{10}$ formation of Ru–P bonds in a molten polyselenophosphate flux. *Angew. Chem. Int. Ed*. **1997**, 36, 1324–1326.

(14) Banerjee, S.; Malliakas, C. D.; Jang, J. I.; Ketterson, J. B.; Kanatzidis, M. G. $_\infty^2[ZrPSe_6]^-$: a soluble photoluminescent inorganic polymer and strong second harmonic generation response of its alkali salts. *J. Am. Chem. Soc*. **2008**, 130, 12270–12272.

(15) Brockner, W.; Becker, R.; Eisenmann, B.; Schäfer, H. Kristallstruktur und schwingungsspektren der caesium-und kalium-hexathiometadiphosphate $Cs_2P_2S_6$ und $K_2P_2S_6$. *Z. Anorg. Allg. Chem*. **1985**, 520, 51–58.

(16) Liao, J. H.; Varotsis, C.; Kanatzidis, M. G. Syntheses, structures, and properties of six novel alkali metal tin sulfides: $K_2Sn_2S_8$, alpha.-$Rb_2Sn_2S_8$, beta.-$Rb_2Sn_2S_8$, $K_2Sn_2S_5$, $Cs_2Sn_2S_6$, and Cs_2SnS_{14}. *Inorg. Chem*. **1993**, 32, 2453–2462.

(17) Kanatzidis, M. G.; Park, Y. Molten salt synthesis of low-dimensional ternary chalcogenides: novel structure types in the K/Hg/Q system (Q = S, Se). *Chem. Mater*. **1990**, 2, 99–101.

(18) Liao, J. H.; Varotsis, C.; Kanatzidis, M. G. Quaternary rubidium copper tin sulfides $Rb_2Cu_2SnS_4$, $A_2Cu_2Sn_2S_6$ (A = Na, K, Rb, Cs), $A_2Cu_2Sn_2Se_6$ (A = K, Rb), potassium gold tin sulfides, $K_2Au_2SnS_4$, and $K_2Au_2Sn_2S_6$. Syntheses, structures, and properties of new solid-state chalcogenides based on tetrahedral $[SnS_4]^{4-}$ units. *Chem. Mater*. **1993**, 5, 1561–1569.

(19) Knaust, J. M.; Dorhout, P. K. Synthesis and structures of $Na_4P_2Se_6$, Cs_3PSe_4, and $Rb_4P_2Se_9$. *J. Chem. Crystallogr*. **2006**, 36, 217–223.

(20) Chondroudis, K.; Kanatzidis, M. G.; Sayettat, J.; Jobic, S.; Brec, R. Palladium chemistry in molten alkali metal polychalcophosphate fluxes: synthesis and characterization of $K_4Pd(PS_4)_2$, $Cs_4Pd(PSe_4)_2$, $Cs_{10}Pd(PSe_4)_4$, $KPdPS_4$, $K_2PdP_2S_6$, and $Cs_2PdP_2Se_6$. *Inorg. Chem*. **1997**, 36, 5859–5868.

(21) Francisco, R. H. P.; Tepe, T.; Eckert, H. A study of the system Li–P–Se. *J. Solid State Chem*. **1993**, 107, 452–459.

(22) McCarthy, T. J.; Kanatzidis, M. G. Synthesis in molten alkali metal polyselenophosphate fluxes: a new family of transition metal selenophosphate compounds, $A_2MP_2Se_6$ (A = K, Rb, Cs; M = Mn, Fe) and $A_2M'P_2Se_6$ (A = K, Cs; M′ = Cu, Ag). *Inorg. Chem*. **1995**, 34, 1257–1267.

(23) Jandali, M. Z.; Eulenberger, G.; Hahn, H. Die kristallstrukturen von $Hg_2P_2S_6$ und $Hg_2P_2Se_6$. *Z. Anorg. Allg. Chem*. **1978**, 447, 105–118.

(24) Chondroudis, K.; McCarthy, T. J.; Kanatzidis, M. G. Chemistry in molten alkali metal polyselenophosphate fluxes, influence of flux composition on dimensionality: layers and chains in $APbPSe_4$, $A_4Pb(PSe_4)_2$ (A = Rb, Cs), and $K_4Eu(PSe_4)_2$. *Inorg. Chem*. **1996**, 35, 840–844.

(25) Gave, M. A.; Canlas, C. G.; Chung, I.; Iyer, R. G.; Kanatzidis, M. G.; Weliky, D. P. $Cs_4P_2Se_{10}$: a new compound discovered with the application of solid-state and high temperature NMR. *J. Solid State Chem*. **2007**, 180, 2877–2884.

(26) Chung, I.; Holmes, D.; Weliky, D. P.; Kanatzidis, M. G. $[P_3Se_7]^{3-}$: a phosphorus-rich square-ring selenophosphate. *Inorg. Chem*. **2010**, 49, 3092–3094.

(27) Chung, I.; Karst, A. L.; Weliky, D. P.; Kanatzidis, M. G. $[P_6Se_{12}]^{4-}$: a phosphorus-rich selenophosphate with low-valent P centers. *Inorg. Chem*. **2006**, 45, 2785–2787.

(28) Chondroudis, K.; Kanatzidis, M. G. $[P_8Se_{18}]^{6-}$: a new oligomeric selenophosphate anion with P^{4+} and P^{3+} centers and pyramidal $[PSe_3]$ fragments. *Inorg. Chem*. **1998**, 37, 2582–2584.

(29) Becker, R.; Brockner, W.; Schäfer, H. Kristallstruktur und schwingungsspektren des di-blei-hexaselenohypodiphosphates $Pb_2P_2Se_6$/crystal structure and vibrational spectra of $Pb_2P_2Se_6$. *Z. Naturforsch.* **1984**, 39, 357–361.

(30) Israel, R.; De Gelder, R.; Smits, J. M. M.; Beurskens, P. T.; Eijt, S. W. H.; Rasing, T.; Van Kempen, H.; Maior, M. M.; Motrija, S. F. Crystal structures of di-tin-hexa(seleno)hypodiphosphate, $Sn_2P_2Se_6$, in the ferroelectric and para-electric phase. *Z. Kristallogr.* **1998**, 213, 34–41.

(31) Jörgens, S.; Mewis, A.; Hoffmann, R. D.; Poettgen, R.; Mosel, B. D. New hexachalcogeno-hypodiphosphates of alkaline-earth metals and europium. *Z. Anorg. Allg. Chem*. **2003**, 629, 429–433.

(32) Chan, B. C.; Feng, P. L.; Hulvey, Z.; Dorhout, P. K. Crystal structure of tetrapotassium hexaselenidohypodiphosphate, $K_4P_2Se_6$. *Z. Krist-new Cryst. St.* **2005**, 220, 9–10.

(33) Toffoli, P.; Khodadad, P.; Rodier, N. Crystal-structure of silver hexaselenohypodiphosphate, $Ag_4P_2Se_6$. *Acta Crystallogr. B* **1978**, 34, 1779−1781.

(34) Brockner, W.; Ohse, L.; Pätzmann, U.; Eisenmann, B.; Schäfer, H. Crystal structure of tetrapotassium hexaselenidohypodiphosphate, $K_4P_2Se_6$. *Z. Krist-new Cryst. St*. **1985**, 40a, 1248–1252.

(35) Coste, S.; Kopnin, E.; Evain, M.; Jobic, S.; Brec, R.; Chondroudis, K.; Kanatzidis, M. G. Polychalcogenophosphate flux synthesis of 1*D*-$KInP_2Se_6$ and 1*D* and 3*D*-$NaCrP_2S_6$. *Solid State Sci.* **2002**, 4, 709–716.

(36) Syrigos, J. C.; Kanatzidis, M. G. Scandium selenophosphates: structure and properties of $K_4Sc_2(PSe_4)_2(P_2Se_6)$. *Inorg. Chem.* **2016**, 55, 4664–4668.

(37) Chondroudis, K.; Kanatzidis, M. G. $K_4In_2(PSe_5)_2(P_2Se_6)$ and $Rb_3Sn(PSe_5)(P_2Se_6)$: one-dimensional compounds with mixed selenophosphate anions. *J. Solid State Chem.* **1998**, 136, 79–86.

(38) Rothenberger, A.; Wang, H.; Chung, D.; Kanatzidis, M. G. Structural diversity by mixing chalcogen atoms in the chalcophosphate system K/In/P/Q (Q = S, Se). *Inorg. Chem.* **2010**, 49, 1144–1151.

(39) Chondroudis, K.; Kanatzidis, M. G. New lanthanide selenophosphates. Influence of flux composition on the distribution of $[PSe_4]^{3-}/[P_2Se_6]^{4-}$ units and the stabilization of the low-dimensional compounds $A_3REP_2Se_8$, and $A_2(RE)P_2Se_7$ (A = Rb, Cs; RE = Ce, Gd). *Inorg. Chem.* **1998**, 37, 3792–3797.

(40) Aitken, J. A.; Evain, M.; Iordanidis, L.; Kanatzidis, M. G. $NaCeP_2Se_6$, $Cu_{0.4}Ce_{1.2}P_2Se_6$, $Ce_4(P_2Se_6)_3$, and the incommensurately modulated $AgCeP_2Se_6$: new selenophosphates featuring the ethane-like $[P_2Se_6]^{4-}$ anion. *Inorg. Chem.* **2002**, 41, 180–191.

(41) Evenson IV, C. R.; Dorhout, P. K. Selenophosphate phase diagrams developed in conjunction with the synthesis of the new compounds $K_2La(P_2Se_6)_{1/2}(PSe_4)$, $K_3La(PSe_4)_2$, $K_4La_{0.67}(PSe_4)_2$, $K_{9-x}La_{1+x/3}(PSe_4)_4$ ($x = 0.5$), and $KEuPSe_4$. *Inorg. Chem.* **2001**, 40, 2875–2883.

(42) Chung, I.; Biswas, K.; Song, J. H.; Androulakis, J.; Chondroudis, K.; Paraskevopoulos, K. M.; Freeman, A. J.; Kanatzidis, M. G. $Rb_4Sn_5P_4Se_{20}$: a semimetallic selenophosphate. *Angew. Chem. Int. Ed.* **2011**, 50, 8834–8838.

(43) Briggs Piccoli, P. M.; Abney, K. D.; Schoonover, J. R.; Dorhout, P. K. Synthesis and structural characterization of quaternary thorium selenophosphates: $A_2ThP_3Se_9$ (A = K, Rb) and $Cs_4Th_2P_5Se_{17}$. *Inorg. Chem.* **2000**, 39, 2970–2976.

(44) Klingen, W.; Eulenberger, G.; Hahn, H. Uber die kristallstrukturen von $Fe_2P_2Se_6$ und $Fe_2P_2S_6$. *Z. Anorg. Allg. Chem.* **1973**, 401, 97–112.

(45) Jörgens, S.; Mewis, A. Die kristallstrukturen von hexachalcogeno-hypodiphosphaten des magnesiums und zinks. *Z. Anorg. Allg. Chem.* **2004**, 630, 51–57.

(46) McCarthy, T. J.; Kanatzidis, M. G. Coordination chemistry of $[P_2Se_6]^{4-}$ in molten fluxes: isolation of the structurally complex KMP_2Se_6 (M = Sb, Bi). *J. Chem. Soc., Chem. Commun.* **1994**, 1089–1090.

(47) Chung, I.; Kanatzidis, M. G. Stabilization of Sn^{2+} in $K_{10}Sn_3(P_2Se_6)_4$ and $Cs_2SnP_2Se_6$ derived from a basic flux. *Inorg. Chem.* **2011**, 50, 412–414.

(48) Kanatzidis, M. G. New directions in synthetic solid state chemistry: chalcophosphate salt fluxes for discovery of new multinary solids. *Curr. Opin. Solid State Mater. Sci.* **1997**, 2, 139–149.

(49) Lin, H.; Chen, L.; Zhou, L. J.; Wu, L. M. Functionalization based on the substitutional flexibility: strong middle IR nonlinear optical selenides $AX^{II}_4X^{III}_5Se_{12}$. *J. Am. Chem. Soc.* **2013**, 135, 12914–12921.

(50) Lin, H.; Liu, Y.; Zhou, L. J.; Zhao, H. J.; Chen, L. Strong infrared NLO tellurides with multifunction: $CsX^{II}_4In_5Te_{12}$ (X^{II} = Mn, Zn, Cd). *Inorg. Chem.* **2016**, 55, 4470–4475.

(51) Yu, P.; Zhou, L. J.; Chen, L. Noncentrosymmetric inorganic open-framework chalcohalides with strong middle IR SHG and red emission: $Ba_3AGa_5Se_{10}Cl_2$ (A = Cs, Rb, K). *J. Am. Chem. Soc.* **2012**, 134, 2227–2235.

(52) Li, Y. Y.; Liu, P. F.; Lin, H.; Wang, M. T.; Chen, L. The effect of indium substitution on the structure and NLO properties of $Ba_6Cs_2Ga_{10}Se_{20}Cl_4$. *Inorg. Chem. Front.* **2016**, 3, 952–958.

(53) Zheng, Y. J.; Liu, P. F.; Wu, X. T.; Wu, L. M.; Lin, H. Synthesis, crystal structure, physical properties and theoretical studies of new ternary sulfide with closed cavities: $CsYb_7S_{11}$. *Chin. J. Struct. Chem.* **2017**, 36, 1780–1790.

(54) Lin, H.; Chen, H.; Liu, P. F.; Yu, J. S.; Zheng, Y. J.; Khan, M. A.; Chen, L.; Wu, L. M. Syntheses, structures, physical and electronic properties of quaternary semiconductors: $Cs[RE_9Cd_4Se_{18}]$ (RE = Tb-Tm). *Dalton Trans.* **2016**, 45, 5775–5782.

(55) Lin, H.; Chen, H.; Lin, Z. X.; Zhao, H. J.; Liu, P. F.; Yu, J. S.; Chen, L.$(Cs_6Cl)_6Cs_3[Ga_{53}Se_{96}]$: a unique long period-stacking structure of layers made from Ga_2Se_6 dimers via cis or trans intralayer linking. *Inorg. Chem.* **2016**, 55, 1014–1016.

(56) Lin, H.; Chen, H.; Zheng, Y. J.; Yu, J. S.; Wu, X. T.; Wu, L. M. Coexistence of strong second harmonic generation response and wide band gap in $AZn_4Ga_5S_{12}$ (A = K, Rb, Cs) with 3D diamond-like frameworks. *Chem.-Eur. J.* **2017**, 23, 10407–10412.

(57) Lin, H.; Zhou, L. J.; Chen, L. Sulfides with strong nonlinear optical activity and thermochromism: $ACd_4Ga_5S_{12}$ (A = K, Rb, Cs). *Chem. Mater.* **2012**, 24, 3406–3414.

(58) Lin, H.; Chen, H.; Zheng, Y. J.; Yu, J. S.; Wu, L. M. $AX^{II}_4X^{III}_5Te_{12}$ (A = Rb, Cs; X^{II} = Mn, Zn, Cd; X^{III} = Ga, In): quaternary semiconducting tellurides with very low thermal conductivities. *Dalton Trans.* **2016**, 45, 17606–17609.

(59) Huang-Fu, S. X.; Shen, J. N.; Lin, H.; Chen, L.; Wu, L. M. Supercubooctahedron $(Cs_6Cl)_2Cs_5[Ga_{15}Ge_9Se_{48}]$ exhibiting both cation and anion exchange. *Chem. Eur. J.* **2015**, 21, 9809–9815.

(60) Lin, H.; Chen, L.; Yu, J. S.; Chen, H.; Wu, L. M. Infrared SHG materials CsM_3Se_6 (M = Ga/Sn, In/Sn): phase matchability controlled by dipole moment of the asymmetric building unit. *Chem. Mater*. **2017**, 29, 499–503.

(61) Lin, H.; Li, L. H.; Chen, L. Diverse closed cavities in condensed rare earth metal-chalcogenide matrixes: $Cs[Lu_7Q_{11}]$ and $(ClCs_6)[RE_{21}Q_{34}]$ (RE = Dy, Ho; Q = S, Se, Te). *Inorg. Chem.* **2012**, 51, 4588–4596.

(62) Lin, H.; Zheng, Y. J.; Chen, H.; Hu, X. N.; Yu, J. S.; Wu, L. M. Non-centrosymmetric selenides $AZn_4In_5Se_{12}$ (A = Rb, Cs): synthesis, characterization and nonlinear optical properties. *Chem.-Asian J.* **2017**, 12, 453–458.

(63) Lin, H.; Shen, J. N.; Chen, L.; Wu, L. M. Quaternary supertetrahedra-layered telluride $CsMnInTe_3$: why does this type of chalcogenide tilt? *Inorg. Chem*. **2013**, 52, 10726–10728.

(64) Lin, H.; Shen, J. N.; Shi, Y. F.; Li, L. H.; Chen, L. Quaternary rare-earth selenides with closed cavities: $Cs[RE_9Mn_4Se_{18}]$ (RE = Ho-Lu). *Inorg. Chem. Front*. **2015**, 2, 298–305.

(65) Lin, H.; Chen, H.; Yu, J. S.; Zheng, Y. J.; Liu, P. F.; Muhammad, A. K.; Wu, L. M. $CsBi_4Te_6$: a new facile synthetic method and mid-temperature thermoelectric performance. *Dalton Trans*. **2016**, 45, 11931–11934.

(66) Lin, H.; Chen, H.; Zheng, Y. J.; Yu, J. S.; Wu, X. T.; Wu, L. M. Two excellent phase-matchable infrared nonlinear-optical materials based on the 3*D* diamond-like frameworks: $RbGaSn_2Se_6$ and $RbInSn_2Se_6$. *Dalton Trans*. **2017**, 46, 7714–7721.

(67) Zheng, Y. J.; Shi, Y. F.; Tian, C. B.; Lin, H.; Wu, L. M.; Wu, X. T.; Zhu, Q. L. An unprecedented pentanary chalcohalide with the Mn atoms in two chemical environments: unique bonding characteristics and magnetic properties. *Chem. Commun*. **2019**, 55, 79–82.

(68) Chen, H.; Liu, P. F.; Lin, H.; Wu, L. M.; Wu, X. T. Solid-state preparation, structural characterization, physical properties and theoretical studies of a series of novel rare-earth metal-chalcogenides with unprecedented closed cavities. *Cryst. Growth Des*. **2019**, 19, 444–452.

(69) Wang, P.; Lin, H. Synthesis, structure, and property of a three-dimensional channel quaternary compound: $Cs_{0.75(6)}Er_{4.43(5)}In_{3.32(6)}S_{12}$. *Chin. J. Struct. Chem.* **2013**, 32, 1873–1879.

(70) Haynes, A. S.; Lee, K.; Kanatzidis, M. G. One-dimensional zinc selenophosphates: $A_2ZnP_2Se_6$ (A = K, Rb, Cs). *Z. Anorg. Allg. Chem*. **2016**, 642, 1120−1125.

(71) *Crystal Clear*, Version 1. 3. 5; Rigaku Corp., Woodlands, TX **1999**.

(72) Sheldrick, G. M. A short history of SHELX. *Acta Crystallogr., Sect. A: Found. Crystallogr.* **2008**, 64, 112−122.

(73) Gelato, L. M.; Parthe, E. STRUCTURE TIDY - a computer program to standardize crystal structure data. *J. Appl. Crystallogr*. **1987**, 20, 139–143.

(74) Kortüm, G. *Reflectance Spectroscopy*, Springer-Verlag, New York **1969**.

(75) Kresse, G.; Furthmüller, J. Efficient iterative schemes for *ab initio* total-energy calculations using a plane-wave basis set. *Phys. Rev. B: Condens. Matter Mater. Phys*. **1996**, 54, 11169−11186.

(76) Kresse, G.; Joubert, D. From ultrasoft pseudopotentials to the projector augmented-wave method. *Phys. Rev. B: Condens. Matter Mater. Phys*. **1999**, 59, 1758−1775.

(77) Perdew, J. P.; Wang, Y. Accurate and simple analytic representation of the electron-gas correlation energy. *Phys. Rev. B* **1992**, 45, 13244−13249.

(78) Perdew, J. P.; Burke, K.; Ernzerhof, M. Generalized gradient approximation made simple. *Phys. Rev. Lett*. **1996**, 77, 3865–3868.

(79) Kanichtschewa, A. S.; Mikhajlov, J. N.; Lazarev, V. B.; Moschchalkova, N. A. Crystal-structure of $CsSbSe_2$. *Dokl. Akad. Nauk*. **1980**, 252, 872−875.

(80) Deiseroth, H. J. Ungewö hnliche lineare, oligomere anionen $(Ga_nSe_{2n+2})^{(n+4)-}$ (n = 2, 4, 6) in festen selenogallaten des casiums. *Z. Kristallogr*. **1984**, 166, 283−295.

(81) Shi, Y. F.; Li, X. F.; Zhang, Y. X.; Lin, H.; Ma, Z. J.; Wu, L. M.; Wu, X. T.; Zhu, Q. L. $[(Ba_{19}Cl_4)(Ga_6Si_{12}O_{42}S_8)]$: a two-dimensional wide-band-gap layered oxysulfide with mixed-anion chemical bonding and photocurrent response. *Inorg. Chem*. **2019**, 58, 6588−6592.

(82) Lin, H.; Shen, J. N.; Zhu, W. W.; Liu, Y.; Wu, X. T.; Zhu, Q. L.; Wu, L. M. Two new phases in the ternary RE–Ga–S systems with the unique interlinkage of GaS_4 building units: synthesis, structure, and properties. *Dalton Trans*. **2017**, 46, 13731−13738.

(83) Liu, C.; Hou, P.; Chai, W.; Tian, J.; Zheng, X.; Shen, Y.; Zhi, M.; Zhou, C.; Liu, Y. Hydrazine-hydrothermal syntheses, characterizations and photo-electrochemical properties of two quaternary chalcogenido antimonates (III) $BaCuSbQ_3$ (Q = S, Se). *J. Alloys Compd*. **2016**, 679, 420−425.

(84) Burke, K. Perspective on density functional theory. *J. Chem. Phys*. **2012**, 136, 150901−9.

(85) Christensen, N. E.; Svane, A.; Peltzer, E. L.; Blancá, Y. Electronic and structural properties of SnO under pressure. *Phys. Rev. B: Condens. Matter. Mater. Phys.* **2005**, 72, 014109−7.

(86) Govaerts, K.; Saniz, R.; Partoens, B.; Lamoen, D. van der Waals bonding and the quasiparticle band structure of SnO from first principles. *Phys. Rev. B: Condens. Matter Mater. Phys*. **2013**, 87, 235210−9.